1-D VELOCITY MODEL FOR SYRIA FROM LOCAL EARTHQUAKE DATA AND NEW SEISMICITY MAP IN SYRIA

Rami Ibrahim[*,], Hiroshi Takenaka[***], Mohamad Daoud[*], and Tatsuhiko Hara[****]**

ABSTRACT

We performed inversion of P and S wave arrival time data from a set of 542 events recorded by the Syrian National Seismological Network during 1995-2004 to determine 1-D velocity structure beneath Syria. We determined both P and S wave velocity structures with a set of station corrections. The P wave velocity in the shallow part in the new model is faster than the current model, while the P wave velocity in the lower part of crust in the new model is slower than that in the current model. We performed hypocenter determination using this new velocity model and compared the relocated hypocenters to hypocenters determined for the current crustal model used by National Earthquake Center of Syria. There is a significant difference in the distributions of their focal depths. When the new velocity model is used, the number of the events in the depth range between 0 and 5 km increases, while that in the depth range between 10 and 15 km decreases. The RMSs of the arrival time residuals obtained by the new model are significantly smaller than those obtained by the current model, which suggests that it is possible to improve the accuracy of hypocenter determination using this new velocity model. We find qualitative correlations between the obtained station corrections and surface geology.

INTRODUCTION

The Syrian National Seismological network recorded 2762 seismic events between 1995 and 2004. The National Earthquake Center of Syria located these events using SEISAN program (Havskov and Ottemöller, 2005). The velocity model used for hypocenter determination was constructed based on refraction, reflection, well loggings and gravity data, but seismic data from natural earthquakes were not used. Therefore, the current velocity model may be significantly biased by heterogeneous sampling of the crust and uppermost upper mantle both horizontally and vertically. Lack of a 1-D velocity model for Syria constrained by data from natural earthquakes is the motivation of this research. The appropriate velocity model is necessary for a variety of purposes, including the reliable routine hypocenter determination, seismic tomography, moment tensor inversion and so on.

In the present study, we determined a 1-D velocity model with station corrections by analyzing data from the Syrian National Seismological network. We used the software VELEST (Kissling 1988; Kissling et al., 1994). The procedure to obtain a 1-D velocity model using this software was explained by Kissling et al. (1994) and Kissling (1995).

TECTONIC SETTINGS OF SYRIA

Figure 1 shows the major tectonic units in Syria. There is the Dead Sea fault system ("DSFS" in Fig. 1) in the west of the country; it has experienced a total slip of about 105 km since Miocene (Quennell, 1958). In the middle of Syria, the intracontinental Palmyrides fold thrust belt represents an early Mesozoic rift basin and Cenozoic convergence associated with nearby plate interaction. At its southwestern extremity in Lebanon, the belt is cut off by the DSFS, whereas to the northeast it stretches into the Euphrates graben system. The Palmyrides is situated between two stable tectonic zones. The Aleppo plateau, which is located to the north-west of Palmyrides, is covered by both

[*] National Earthquake Center, Damascus, Syria.[**] Earthquake Research Institute, University of Tokyo, Japan
[***] Department of Earth and Planetary Sciences, Faculty of Sciences, Kyushu University, Japan
[****] International Institute of Seismology and Earthquake Engineering, Building Research Institute, Japan

Paleozoic and Mesozoic sediments and is “a flat raised structure with little deformation relative to intracontinental Palmyrides belt zone” (Best et al. 1990). To the southeast, lies the Rutbah uplift, which Best et al. (1990) described as broad, domal basement structure. Very little deformation is found in the strata of the uplift, except for along the northeastern edge where it trends into the Euphrates depression (Chaimov et al., 1992).

The Euphrates depression is a NNW-trending asymmetric half graben system that deepens to the east. The Euphrates depression has been faulted down relative to the adjacent eastern platform, and the total slip length is 3.5 km. The Abd el Aziz-Sinjar uplift lies to the northeastern part of the Euphrates depression, and is controlled by a major south dipping reverse fault. Sawaf et al. (1993) suggested that Abd el Aziz-Sinjar uplift was a sedimentary basin in Mesozoic which inverted in the Neogene.

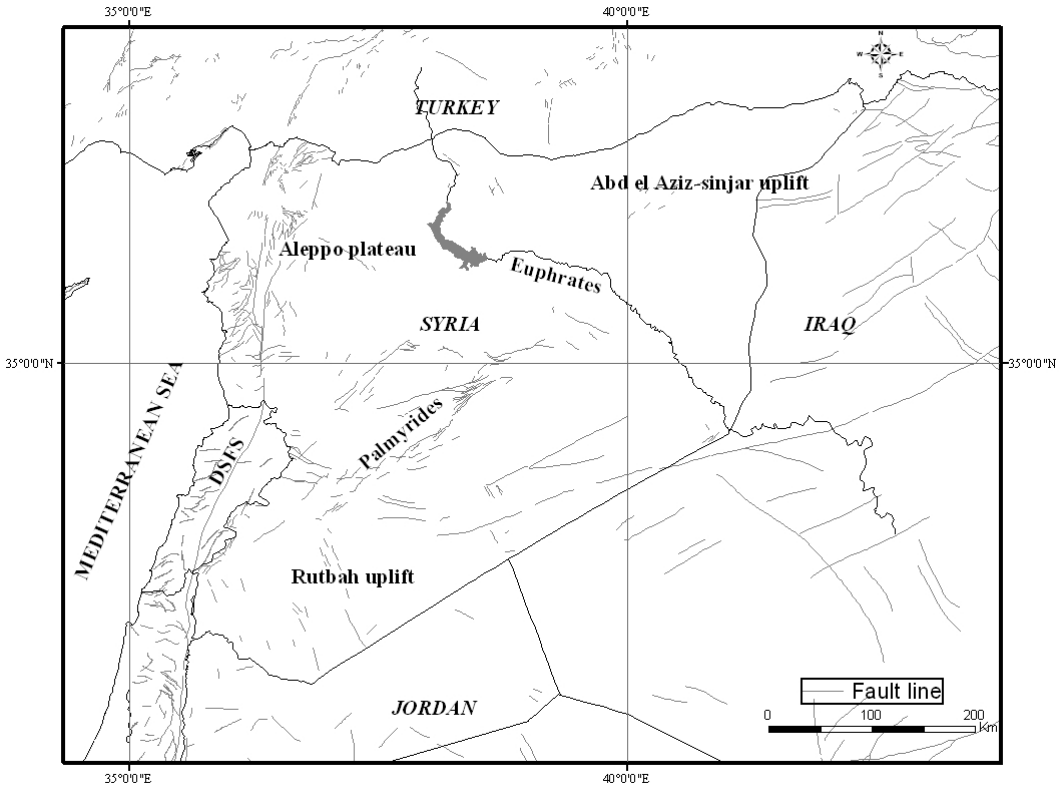

Fig. 1 The major tectonic units in and around Syria. “DSFS” denotes the Dead Sea Fault system.

DATA

The Syrian National Seismological Network has been in operation since 1995. Figure 2 shows the station distribution. The network started with 20 seismic stations with short period sensors with corner frequencies of 1 Hz. The stations have vertical component sensors except stations ARNB, HAWK, RABH, BRBR, ZALF, and WHAB which have three components sensors. These stations were deployed in the western part of the country along the Dead Sea Fault System, which is considered the most seismically active region in the north part of the Arabian Plate. Later in 2003, additional 7 stations (1 Hz short period sensors) were deployed in the north-eastern part of the country to monitor the seismic activity in the Euphrates depression and Abd-el Aziz Sinjar uplift. Among these stations just station SFNE has three components sensor and the rest contains vertical component sensors.

P and S wave arrivals recorded at the Syrian stations were picked manually, and were processed by SEISAN at the National Earthquake Center of Syria. For the present study, from 2,762 earthquakes recorded by the Syrian National Seismological Network, we selected well located 542

earthquakes with a good spatial distribution for the active regions inside and surrounding the country. Figure 3 shows the distribution of the selected events. For each event, we have at least 6 P and S wave arrivals. Figure 4 shows the numbers of P and S arrival time data for each station.

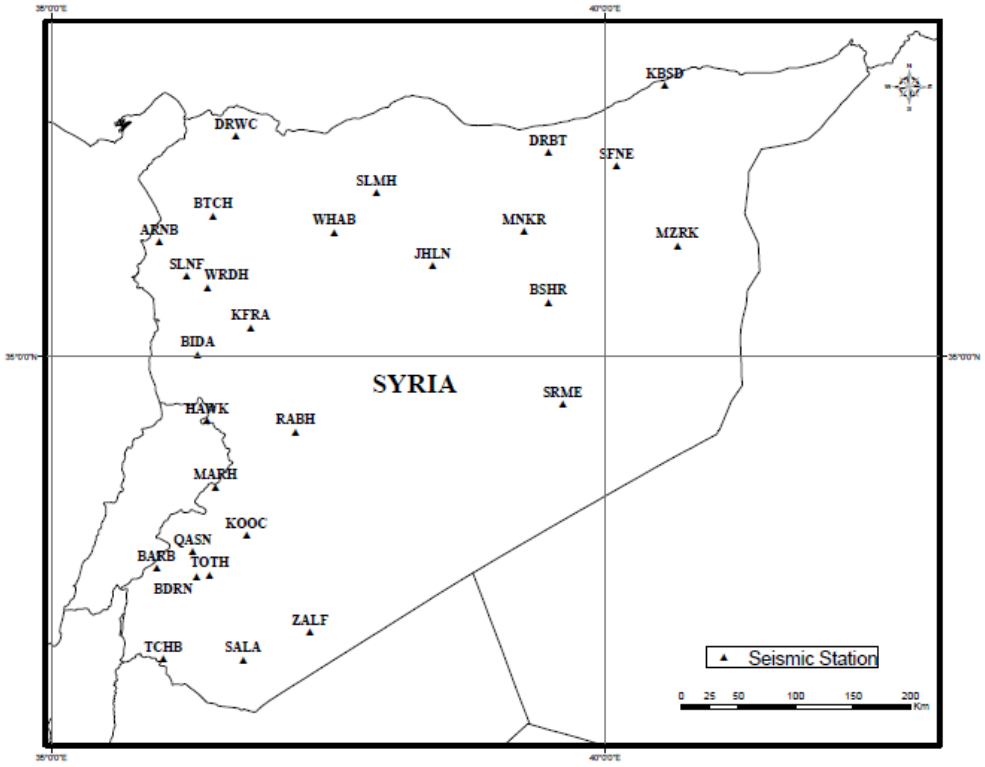

Fig. 2 The distribution of the short period seismic stations of the Syrian National Seismological Network.

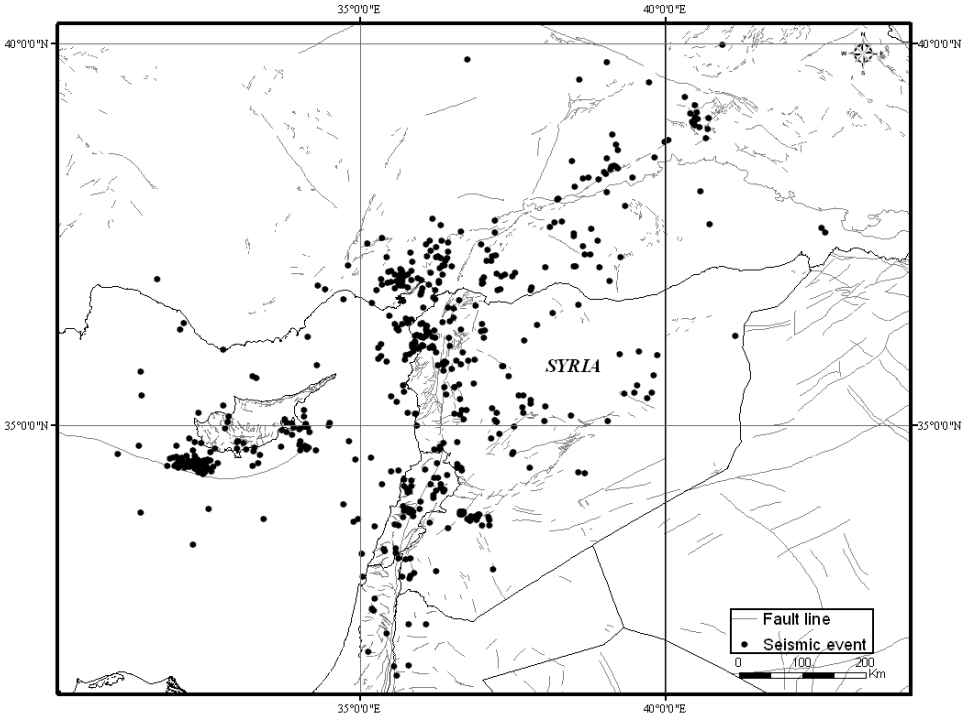

Fig. 3 The distribution of the selected events for this study.

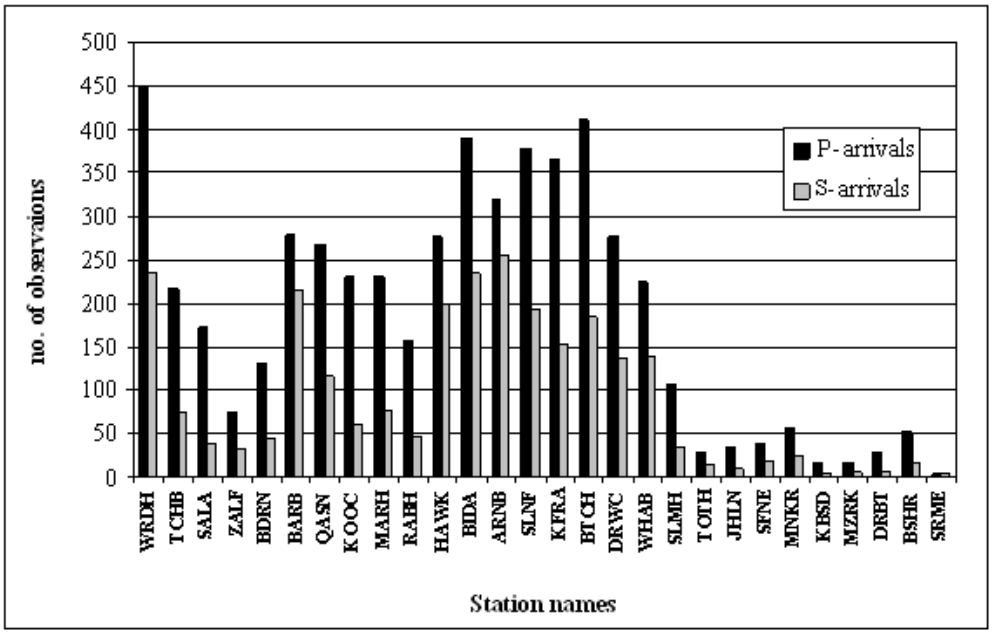

Fig. 4 The number of observations for each station for the 542 selected events. The stations in the right side of the chart have smaller numbers of observations because they have been deployed since 2003. The total numbers of P and S wave arrivals are 5236 and 2582, respectively.

PROCEDURES AND A PRIORI VELOCITY MODEL

Figure 5 shows the data analysis procedure of this study. First we constructed an initial reference velocity model. Since such a velocity model is built based on deep seismic exploration data down to the Moho is not available in Syria, we referred to seismic exploration experiments performed in neighboring countries under geological conditions similar to that of Syria. We found data from two seismic refraction experiments: El-Isa et al. (1987) performed a seismic refraction experiment in the west and middle Jordan to obtain P and S wave velocity models for the crust and uppermost upper mantle; Mechie et al. (2005) obtained P and S wave velocity models based on refraction and reflection explorations across the Dead Sea fault in the west of Jordan and the east of Palestine. Based on these two studies, we constructed our initial reference velocity model shown in Table 1. We used the top layer, for which “Depth to the top of the layer (km)” is negative, to account for station elevations. The minimum focal depth is set to 0 km in this study.

For the velocity inversion it was necessary to choose a reference station, which should have a continuous or nearly continuous record of events. It had to be a reliable station, preferably located near the center of the network, and had not show extreme site effects (Kissling et al., 1994). We have chosen WRDH as a reference station in this study. This station is located in the north-west of the network (Fig. 2) and the site conditions at this station are good (hard limestone rocks from the Cretaceous period). This station has the largest number of P wave arrivals (447 wave arrivals) and a large number of S wave arrival time data (235 wave arrivals).

We performed initial inversion using the initial reference velocity model for the data described in the previous section (we set the maximal epicentral distance for phase use to 500 km). We constructed more detailed velocity model based on the initial velocity model, consisting of 19 layers. Each layer except for the first layer has a thickness of 2 km (Table 2). Then another inversion was carried out using this finer layer velocity model to find the clear sharp velocity changes at depths of 4km, 10km, 18km, and 34 km. For a depth of 10km, only P wave velocity changes, while the velocity changes are found both for P and S waves at the other depths.

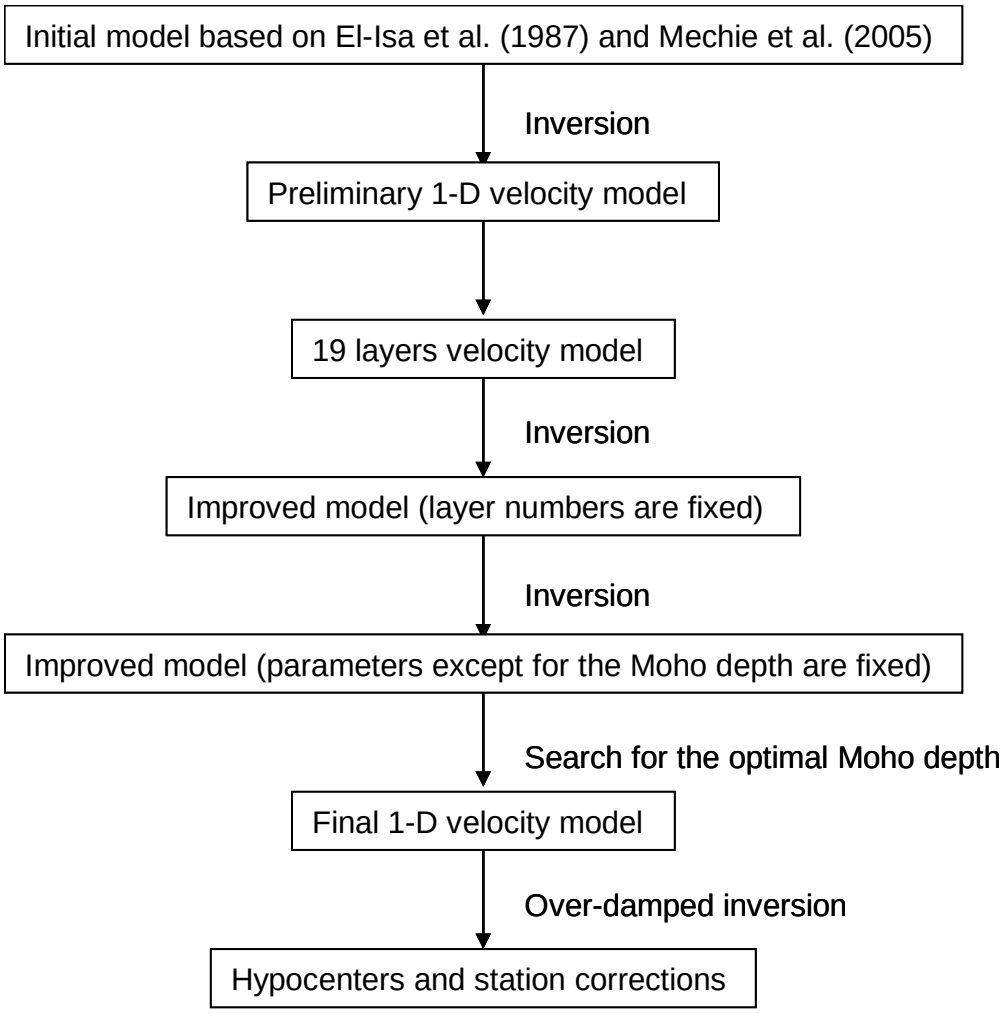

Fig. 5 The flowchart of the procedure to obtain the 1-D velocity model. See the text for details.

Table 1 The initial velocity model based on data from El-ISA et al. (1987) and MECHIE et al. (2005).

Vp (km/sec)	**Vs (km/sec)**	**Depth to the top of the layer (km)**
4.60	2.65	-3
4.60	2.65	0
4.60	2.65	2
6.00	3.64	5
6.30	3.68	10.5
6.40	3.68	18.5
6.65	3.68	20
7.90	4.47	34

Based on this result, we constructed a velocity model consisting of five layers for P wave velocity and four layers for S wave velocity. Then we perform another inversion using this model as a new initial model. Finally, to find the optimal Moho depth, we varied the Moho depths from 30 km to 42 km while fixing the other velocity model parameters. Figures 6 and 7 show the RMSs of the residuals and the S wave station corrections for the reference station as a function of the Moho depths, respectively. The minimum RMS was obtained for a depth of 38 km. The velocity model with the Moho at a depth of 38 km is consistent with the S wave station correction of the reference station, because it is close to zero around this depth. After obtaining this final model, we determined hypocenters and station corrections using this model.

Table 2 The 19 layers velocity model used to search the optimal numbers of layers.

Vp (km/sec)	**Vs (km/sec)**	**Depth to the top of the layer (km)**
5.44	3.14	-3
5.44	3.14	0
5.44	3.14	2
5.44	3.14	4
5.89	3.40	6
5.89	3.40	8
6.25	3.61	10
6.25	3.61	12
6.25	3.61	14
6.25	3.61	16
6.61	3.82	18
6.61	3.82	20
6.61	3.82	22
6.61	3.82	24
6.61	3.82	26
6.61	3.82	28
6.61	3.82	30
6.61	3.82	32
7.95	4.57	34
7.95	4.57	36

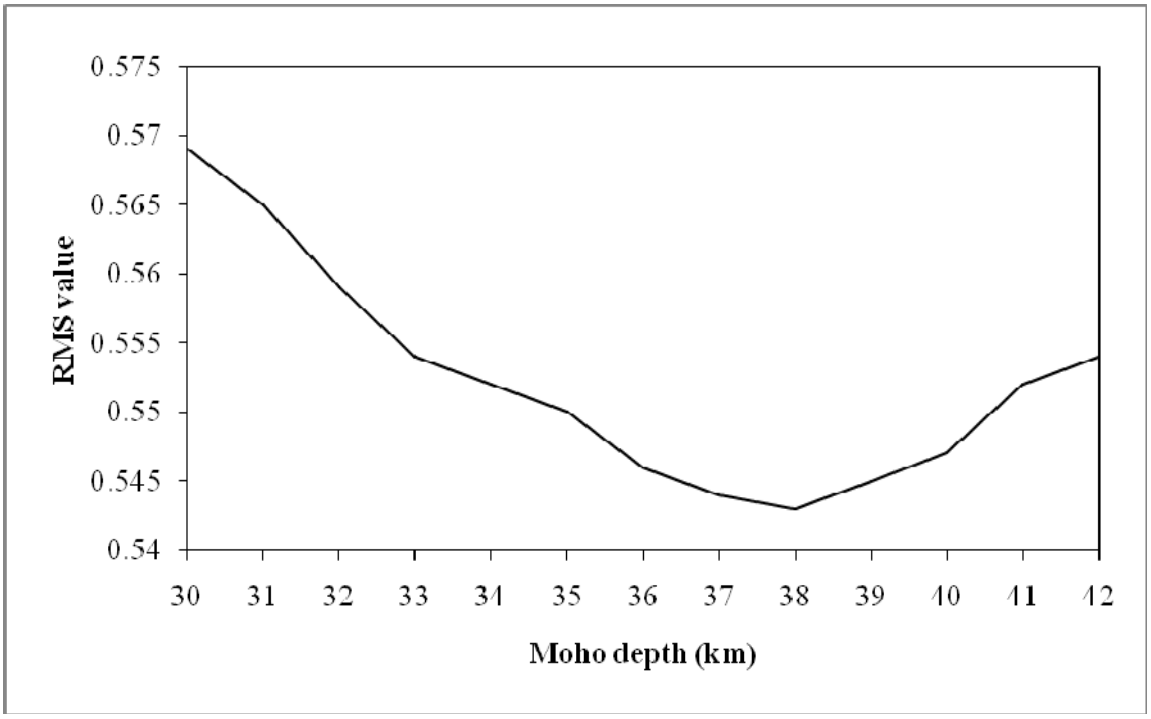

Fig. 6 The RMSs as a function of Moho depths. The depth of 38 km provides the minimum RMS (0.543).

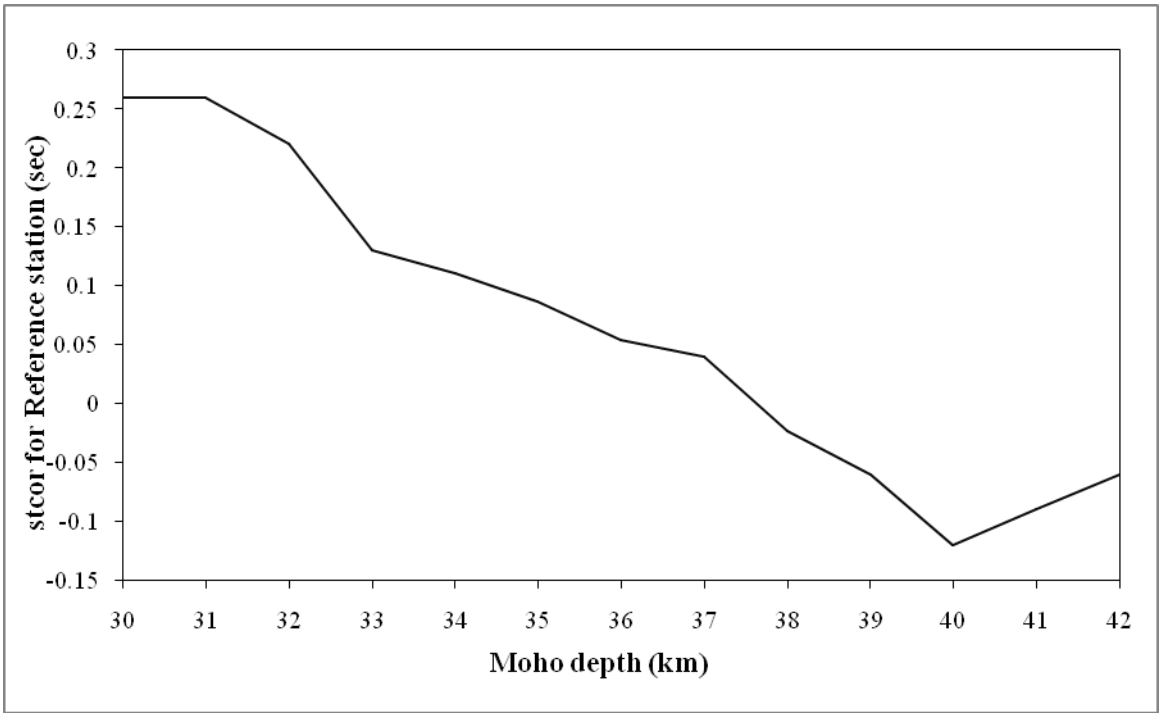

Fig. 7 S-wave station correction for the reference station as a function of Moho depths. It is close to 0 s for the depth of 38 km, which provides the minimum RMS as is shown in Fig. 6

RESULTS AND DISCUSSION

Velocity model, relocated hypocenters and arrival time residuals

Figure 8 and Table 3 show the estimated 1-D velocity model and corresponding Vp/Vs ratio. In Fig. 8, we also show the current velocity model used for hypocenter determination by National Earthquake Center of Syria for comparison. The P wave velocity in the shallow part (down to a depth of about 5 km) in our model is faster than the current model. The slow P wave velocity in the current model is likely to come from seismic exploration data. Our result suggests that such low velocity is not representative of the average 1-D velocity model for Syria. The P wave velocity in the lower part of crust in our model is slower than that in the current model. The constraints for this depth range are likely to be weak considering the dataset used in the construction of this model.

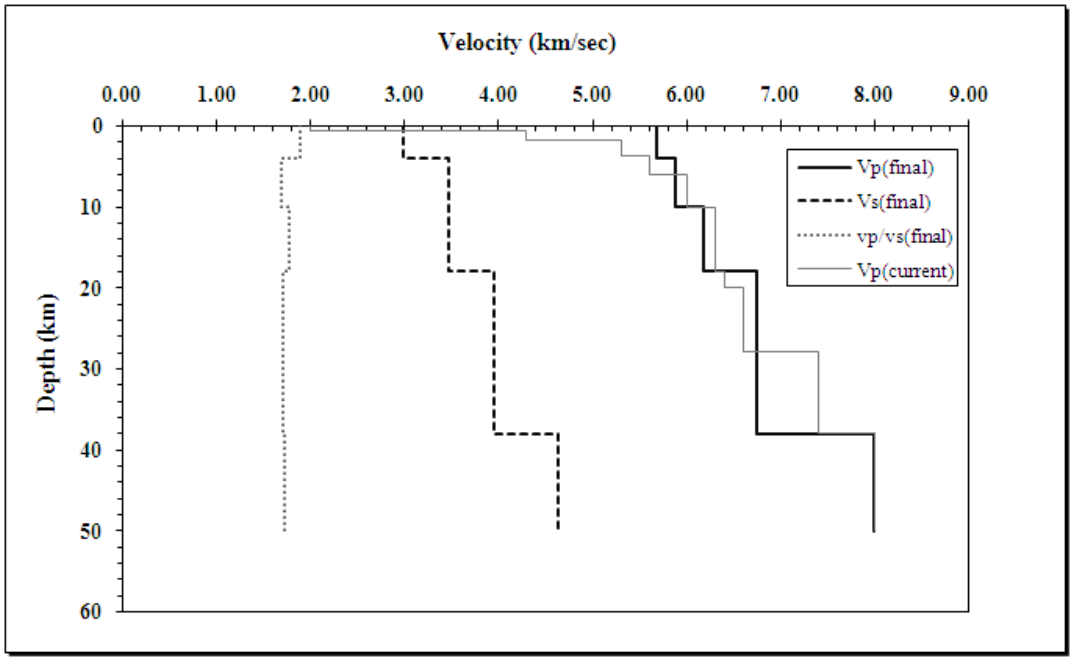

Fig. 8 The final 1-D P and S wave velocity models are shown by the thick solid and dashed lines, respectively. The corresponding Vp/Vs ratio is shown by the dotted line. The current P wave velocity model used by the National Earthquake Center of Syria is shown by the thin solid line for comparison.

Table 3 The final velocity model and Vp/Vs ratio.

Vp (km/sec)	Vs (km/sec)	Vp/Vs	Depth to the top of the of layer (km)
5.67	2.98	1.90	-3
5.68	2.99	1.90	0
5.87	3.48	1.69	4
6.18	3.48	1.78	10
6.74	3.95	1.71	18
8.00	4.64	1.72	38

(a)

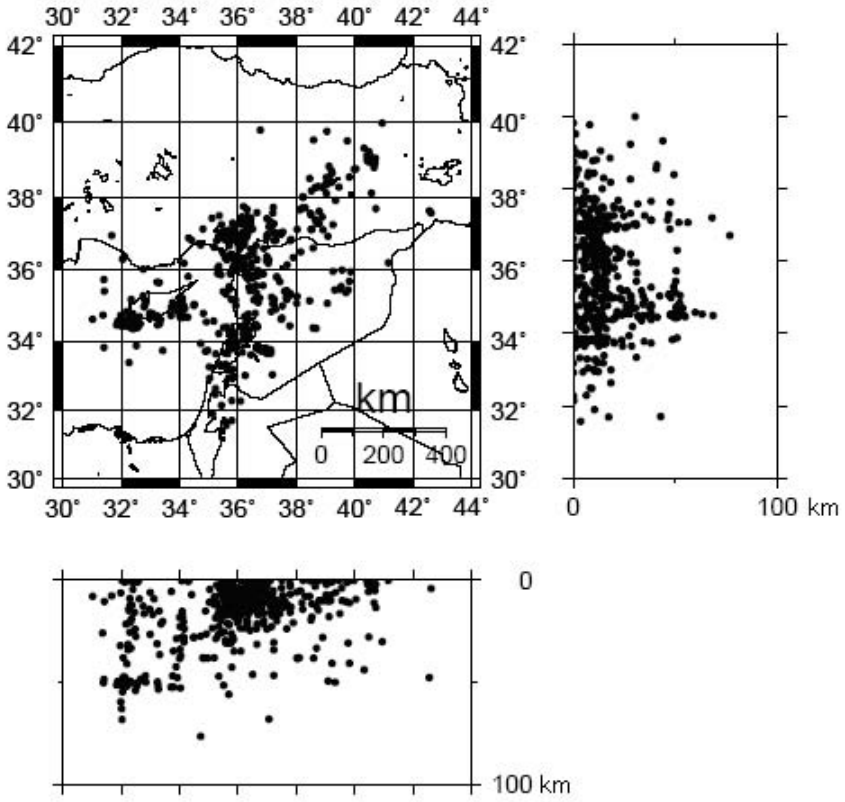
30° 32° 34° 36° 38° 40° 42° 44°
42°
40°
38°
36°
34°
32°
30°
km
0 200 400
0
100 km
0
100 km

(b)

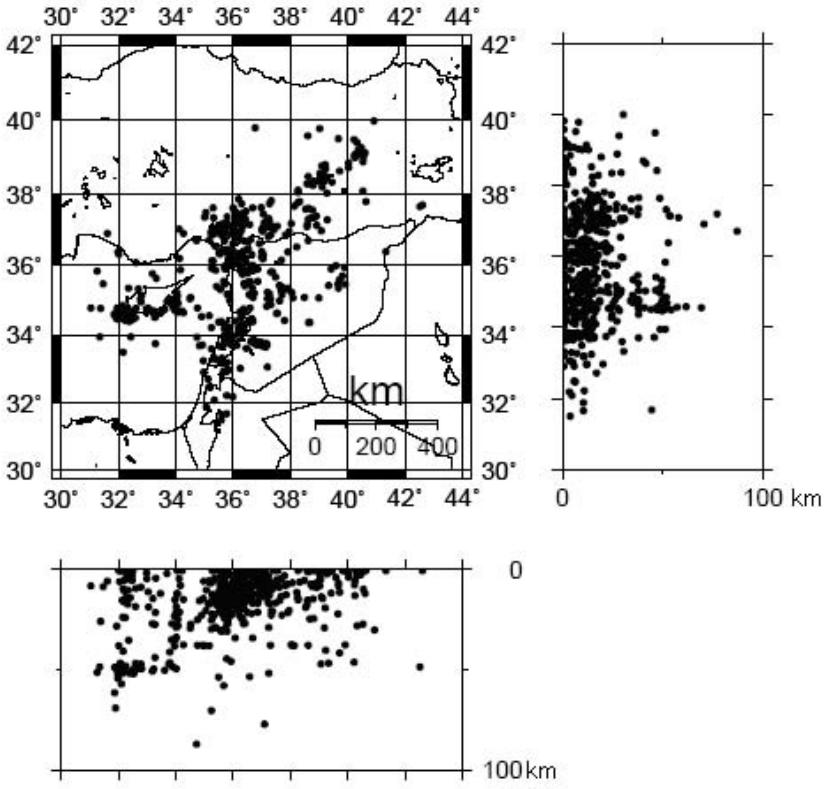
30° 32° 34° 36° 38° 40° 42° 44°
42°
40°
38°
36°
34°
32°
30°
km
0 200 400
0
100 km
0
100 km

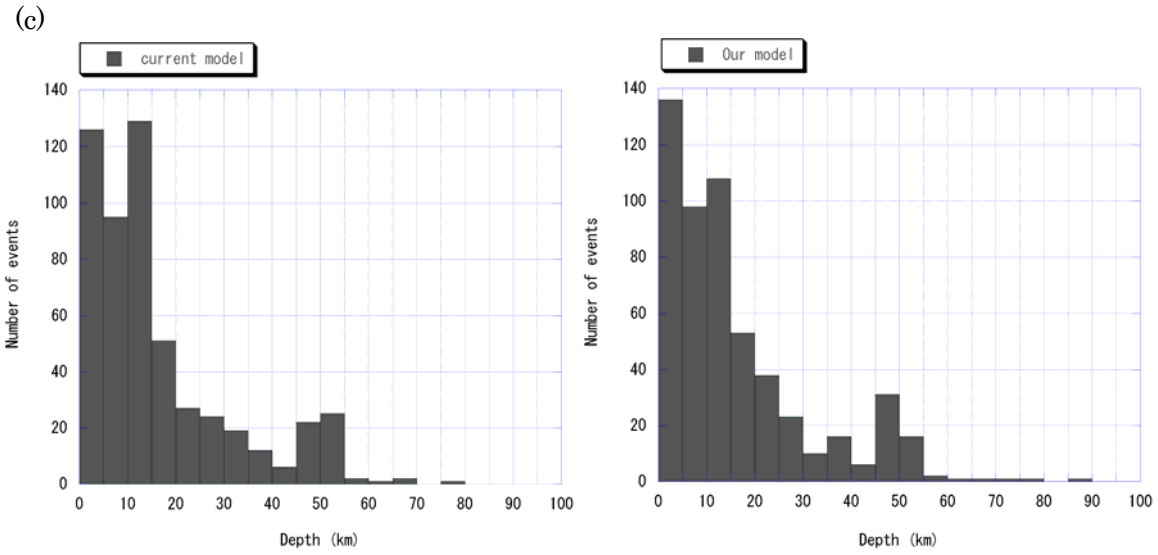

Fig. 9 The hypocenters and frequency distributions of the focal depths of the 542 events used in inversion for 1-D velocity structure. (a) The hypocenters determined by the current velocity model are shown in the map and cross sections in the N-S and E-W directions. (b) The hypocenters determined by the model obtained in this study are shown in the map and cross sections in the N-S and E-W directions. (c) The frequency distributions of the focal depths of the hypocenters shown in (a) (denoted as "current model") and (b) (denoted as "Our model") are shown in the left and right panels, respectively.

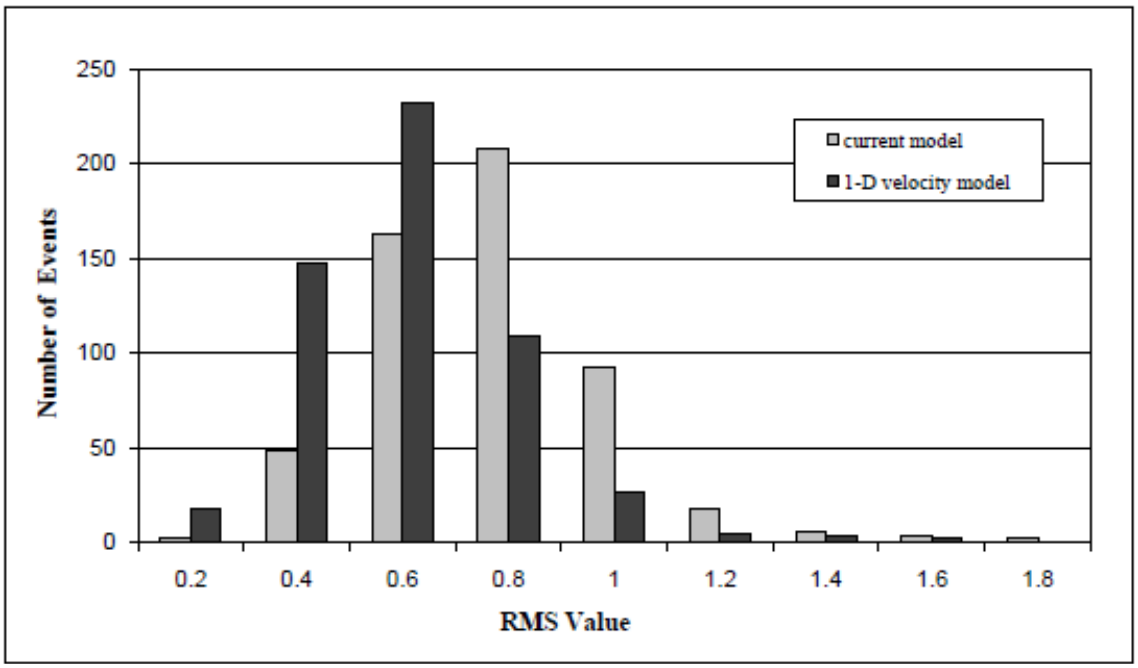

Fig. 10 Frequency distributions of RMSs of arrival time residuals for the events used in this study for the final model (dark gray) and the current model are shown (light gray), respectively.

Figure 9 shows the hypocenters determined by the model obtained in this study and those determined by the current velocity model with their depth distributions. While there is not a large difference between their epicenters, there is a difference between their depth distributions. When our model is used, the number of the events in the depth range between 0 and 5 km increases, while that in the range between 10 and 15 km decreases. This difference can be found in the new seismicity map obtained using our model, which will be presented later.

Figure 10 shows the comparison of the RMSs of the arrival time residuals obtained for our model and those obtained for the current model. Clearly, the residuals of our model are smaller than those of the current model. The averages of the RMSs are 0.70 sec and 0.99 sec for our and current models, respectively. This result means that our model better fits the observed arrival times.

Station corrections

Figure 11 shows the station corrections for P and S waves. In the inversion, only the P wave station correction for the reference station is set to zero. Since we considered the station elevations in the inversion, the obtained station corrections are expected to reflect the effects of near surface geology. For the reference station WRDH, the P wave station correction was set to zero in the inversion, and the S wave station correction is close to zero (0.01 sec), which was shown in the previous section.

The positive P and S wave station corrections are obtained for stations KFRA, BTCH, ARNB, HAWK, SFNE, DRBT and MNKR. They imply lower velocities, which are qualitatively consistent with surface geology. KFRA is on Upper Miocene basalt rocks. They are porous and also highly weathered. BTCH is on Middle Miocene rocks, which are characterized by soft chalky and firm nummulitic limestone. ARNB is located on Precambrian rocks. The geological structure is complicated, and consists of Serpentinized-Pridotites, Diabases, Spilities, Argillites, Radiolarites, Lava and Tuffs. The surface rocks are highly weathered. HAWK and SFNE are on Cretaceous rocks of limestone interbedded by Marl. DRBT is located on Paleogene rocks characterized by limestones interbedded with Marl. MNKR is in the Upper Quaternary region, and the site itself is located on Tuffs rocks.

Station TCHB has positive P and S wave station corrections. The station site is located on Paleocene and Lower Eocene chalky and nummulitic limestones. The limestones merge with Marls and Clays. The geological complexity is likely to affect the observed station corrections.

Stations SLNF and BARB are located on massive homogenous limestone rocks, which belong to Upper Jurassic. The negative P and S wave station corrections are obtained for this station, which suggests higher velocities beneath them.

The large negative S wave station corrections are obtained for stations KBSD and MZRK. They are located on basaltic rocks, for which higher velocities are expected.

Station SRME shows the relatively large positive P wave station correction and large negative S wave station correction, which are likely to come from the small number of observations for this station (4 P wave arrivals and 3 S wave arrivals).

For Stations RABH, QASN, KOOC, TOTH, BDRN, and BSHR located in and around the Palmyrides fold thrust belt (Fig. 1), the large positive P and S wave station corrections are obtained. Their cause should be investigated in future studies.

New seismicity map of Syria

We relocated the 2762 events recorded by the Syrian National Seismological Network between 1995-2004 using the new velocity model and station corrections obtained in this study. Figure 12 shows the seismicity obtained for the current and new velocity models with their focal depth distributions. In Figure 12(c), we can find the same differences that were mentioned above on the relocated events used in inversion, namely, the increase and decrease in the numbers of events in the depth range between 0 and 5 km and that between 10 and 15 km. As a result, the peak in the depth range between 10 and 15 km disappears in the depth distribution of the relocated events.

In Figure 13, we show the seismicity in the western part of Syria considering its high seismicity and the good station coverage for this part. Again, we find the same differences, which

implies that they are robust. These results will be useful to improve our understanding on the seismic activity and sesimogenesis in Syria, since the focal depth distribution reflects geological and geophysical conditions of faults such as fault develomement, temperature, and so on (e.g., Meissner and Strehlau, 1982; Scholz, 2002), although further accumulation of data and analyses are required.

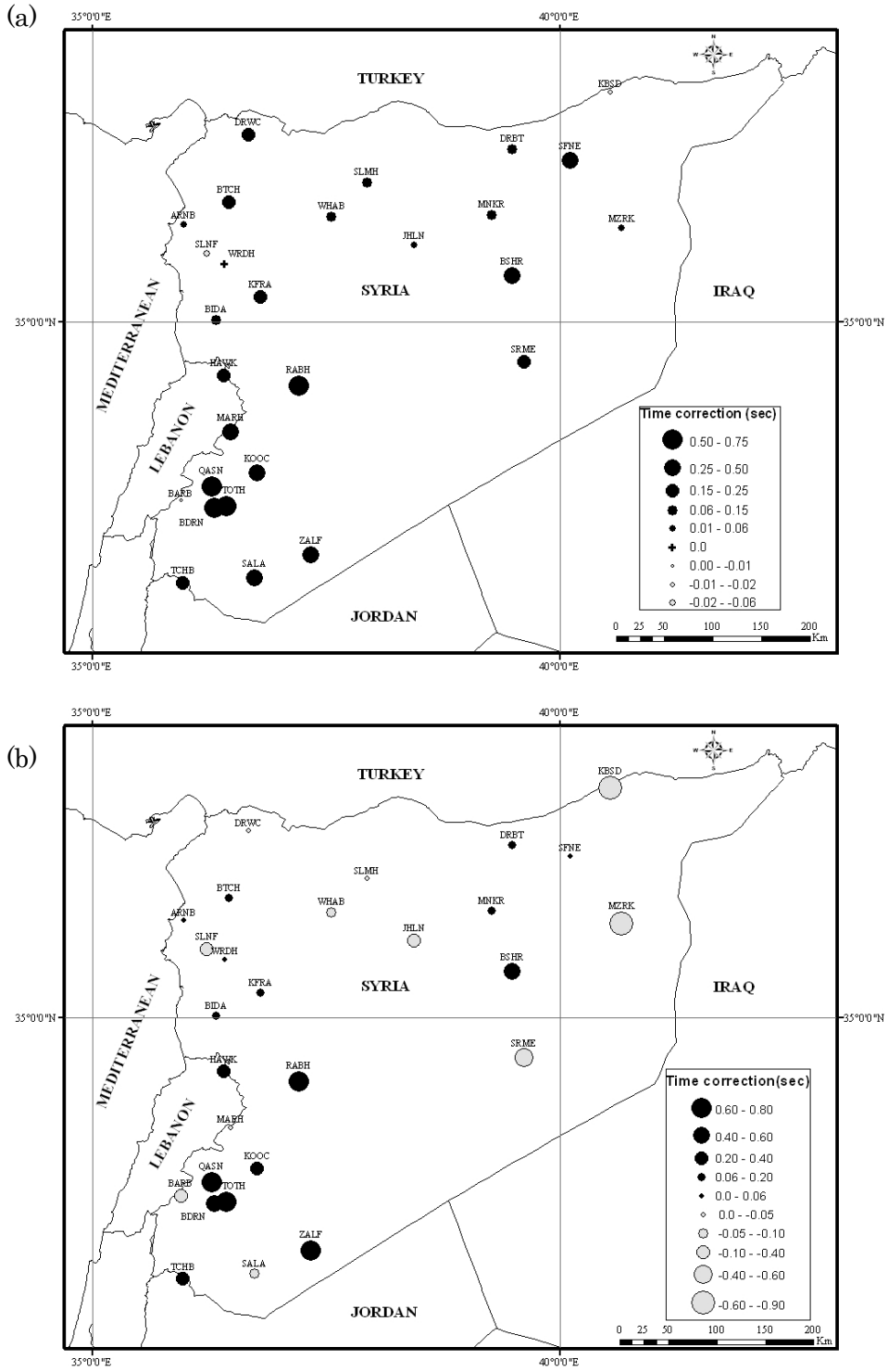

Fig. 11 The station corrections for P waves (a) and S waves (b), respectively. Black and gray circles represent positive and negative corrections, respectively.

(a)

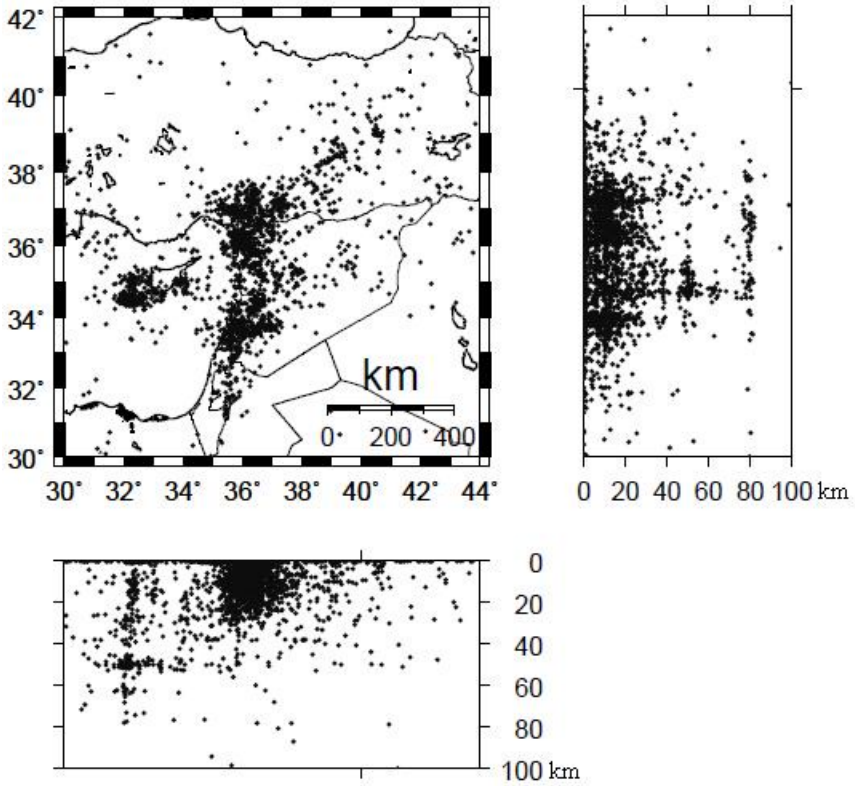
42°
40°
38°
36°
34°
32°
30°
30° 32° 34° 36° 38° 40° 42° 44°
km
0 200 400
0 20 40 60 80 100 km
0
20
40
60
80
100 km

(b)

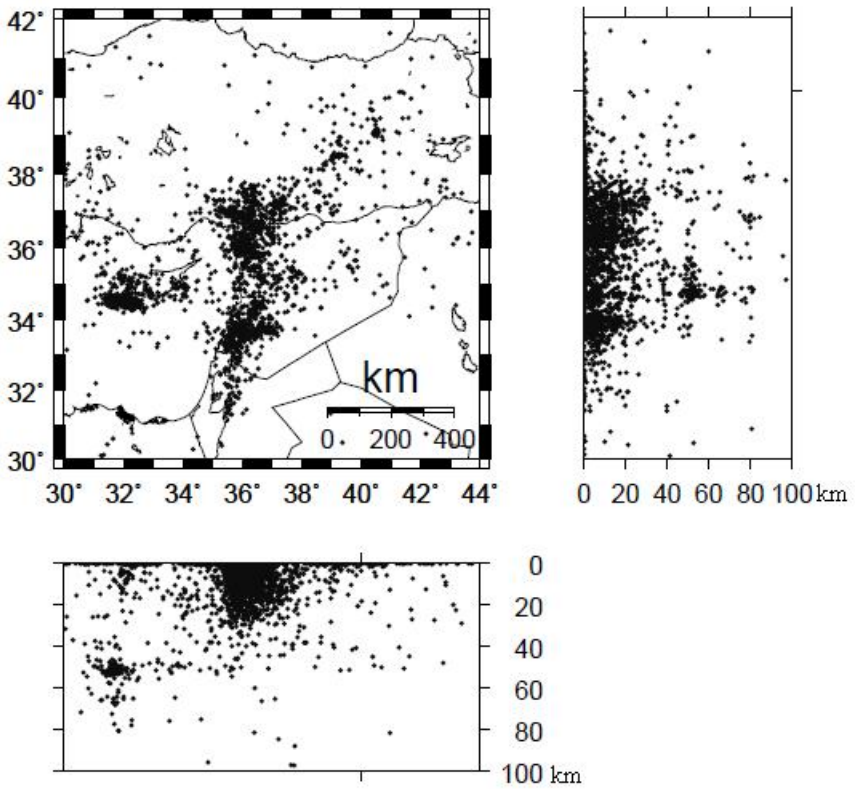
42°
40°
38°
36°
34°
32°
30°
30° 32° 34° 36° 38° 40° 42° 44°
km
0 200 400
0 20 40 60 80 100 km
0
20
40
60
80
100 km

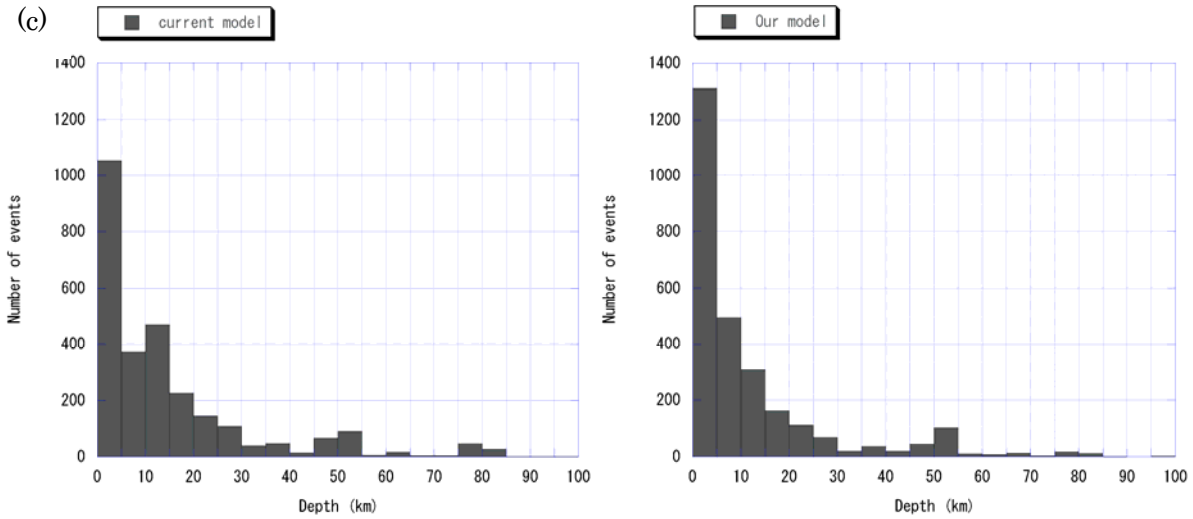

Fig 12. The hypocenters and frequency distributions of the focal depths of the 2762 events recorded by the Syrian National Seismological Network between 1995-2004. (a) The hypocenters determined by the current velocity model are shown in the map and cross sections in the N-S and E-W directions. (b) The hypocenters determined by the model obtained in this study are shown in the map and cross sections in the N-S and E-W directions. (c) The frequency distributions of the focal depths of the hypocenters shown in (a) (denoted as “current model”) and (b) (denoted as “Our model”) are shown in the left and right panels, respectively.

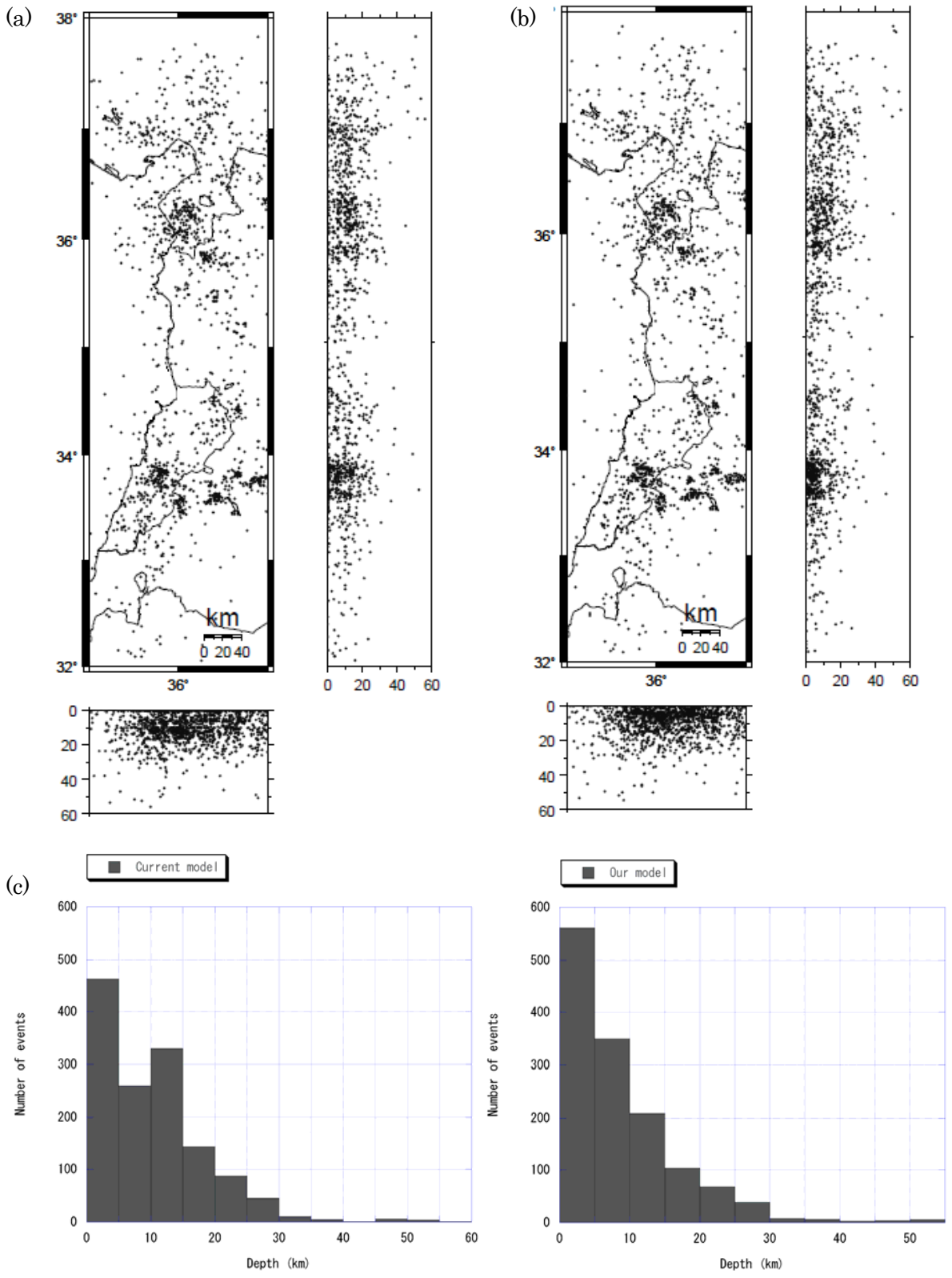

Fig 13. The hypocenters and frequency distributions of the focal depths of the events in the western part of Syria, Lebanon, North Jordan and South Turkey. (a) The hypocenters determined by the current velocity model. (b) The hypocenters determined by the model obtained in this study. (c) The frequency distributions of the focal depths of the hypocenters shown in (a) (denoted as “current model”) and (b) (denoted as “Our model”) are shown in the left and right panels, respectively.

CONCLUDING REMARKS

We performed inversion of P and S wave arrival times from the Syrian National Seismological Network to determine one-dimensional P and S wave velocity structures of the crust and uppermost upper mantle beneath Syria with a set of station corrections. The Moho depth is estimated to be 38 km. The P wave velocity in the shallow part of our model is faster than that in the current model used by National Earthquake Center of Syria, while the P wave velocity in the lower part of the crust in our model is slower. We performed hypocenter determination using this new velocity model and compared the relocated hypocenters to those determined for the current model routinely used by National Earthquake Center of Syria. We found a significant difference in the distributions of their focal depths. When the new model is used, the number of the events whose focal depths are in the range between 0 and 5 km increases, while the number of events whose focal depths are in the range between 10 and 15 km decreases. Our model better explains the observed arrival times. The averages of the RMSs of the arrival time residuals are 0.70 sec and 0.99 sec for the new and current models, respectively. This suggests the possibility to improve the accuracy of hypocenter determination using this new velocity model. We have found qualitative correlations between the station corrections and surface geology.

The velocity model obtained in the present study is the first model of Syria crustal structure based on natural earthquake data recorded in Syria. This new model will be used to locate earthquakes in and around Syria with higher accuracy. An increase of precise hypocenter data will make it possible to perform seismic tomography for the study area in future, where our model may be used as an initial model for such tomographic studies. We hope that our model will be the first step for seismotectonic studies in Syria

ACKNOWLEDGMENTS

This study was started when the first author participated in the JICA training course entitled “Seismology, Earthquake Engineering and Disaster Mitigation” during 2006-2007. We thank the anonymous reviewer for his comments, which were helpful to improve the original manuscript. We are grateful for the National Earthquake Center of Syria for providing us the earthquake data. We thank both Dr. Arash JafarGandomi and Dr. Genti Toyokuni from the seismological laboratory in Kyushu University for their useful discussions. We also thank Dr. Samer Bagh and Ms. Rayan Yasamenh from the National Earthquake Center of Syria for their helps in making some figures using the Generic Mapping Tools (GMT, Wessel and Smith, 1998) and GIS.

REFERENCES

Best, J.A., Barzangi, M., AL-Saad, D., Sawaf, T., and Gebran, A. (1990), Bouguer gravity trends and crustal structure of the Palmyride Mountain belt and surrounding northern Arabian platform in Syria, Geology, 18, 1235-1239.

Chaimov, T.A., Barazangi, M., AL-Saad, D., Sawaf, T., and Gebran, A. (1992), Mesozoic and Cenozoic deformation inferred from seismic stratigraphy in the southwestern intracontinental Palmyride fold-thrust belt, Syria, GSA Bulletin, 104, 704-715.

El-isa, Z., Mechie, J., and Prodehl C. (1987), Shear velocity structure of Jordan from explosion seismic data, Geophys. J. R. astr. Soc., 90, 265-281.

Havskov, J. and Ottemöller, L. (2005), SEISAN: The Earthquake Analysis Software, Version 8.1, Univ. Bergen, Norway.

Kissling, E. (1988), Geotomography with local earthquake data, Rev. Geophys., 26, 659-698.

Kissling, E., Ellsworth, W.L., Eberhart-Phillips, D., and Kradolfer, U. (1994), Initial reference models in local earthquake tomography, J. Geophys. Res., 99, 19,635-19,646.

Kissling, E. (1995), VELEST User’s Guide, Internal report, Institute of Geophysics, ETH Zurich, pp. 26.

Mechie, J., Abu-Ayyash, K., Ben-Avraham, Z., El-kelani, R., Mohsen, A., Rümpker, G., Saul, J., and Weber, M. (2005), Crustal shear velocity structure across the Dead Sea Transform from two-dimensional modelling of DESERT project explosion seismic data, Geophys. J. Int., 160, 910-924, doi: 10.1111/j.1365-246X.2005.02526.x.

Meissner, R. and Strehlau, J. (1982), Limits of stresses in continental crusts and their relation to the depth-frequency distribution of shallow earthquakes, Tectonics, 1, 73–89, doi:10.1029/TC001i001p00073.

Quennell, A.M. (1958), The structural and geomorphic evolution of the Dead Sea rift, Quarterly Journal of Geological Society, 114, 1-24.

Sawaf, T., Al-Saad, D., Gebran, A., Barazangi, M., Best, J.A., and Chaimov, T,A.(1993), Stratigraphy and structure of eastern Syria across the Euphrates depression, Tectonophysics, 220, 267-281.

Scholz, C. H. (2002), The mechanics of earthquakes and faulting, 2nd ed. Cambridge University Press.

Wessel, P. and Smith, W.H.F. (1998), New, improved version of the Generic Mapping Tools released, EOS Trans. AGU, 79(47), 579.